J Fluoresc (2009) 19:221–228
DOI 10.1007/s10895-008-0406-2

ORIGINAL PAPER

Photoluminescence Enhancement Effect of CeO_2 in Rare Earth Composites $MM'O_3/CeO_2$ and $MM'O_3/CeO_2$: Pr^{3+} (M=Ca, Sr; M′=Ti, Zr)

Bing Yan · Xiaowen Cai · Xiuzhen Xiao

Received: 29 February 2008 / Accepted: 28 July 2008 / Published online: 16 August 2008

Abstract In the context, a modified sol-gel technology was afford to the synthesis of rare earth composite ceramic phosphors $MM'O_3/CeO_2$ and $MM'O_3/CeO_2$: Pr^{3+} (M=Ca, Sr; M′=Ti, Zr) with multicomponent hybrid precursors were composed. The micromorphology, particle size and photoluminescence properties were studied with XRD, SEM and luminescent spectroscopy in detail. Both XRD and SEM indicated the particle sizes were in the submicrometer range of 100∼300 nm. The photoluminescence for these ceramic phosphors were studied in details with the different component of host (molecular ratio of Sr, Ca and Ti, Zr), presenting a broad spectral band in the visible blue-violet region with the maximum excitation peak at 449 nm and a wide emission range with a maximum peak at 619 nm, which was ascribed to be the characteristic transition of Pr^{3+} ($^1D_2 \rightarrow {}^3H_4$). These phosphors can be expected for visible light conversion (blue → red) materials. Especially it can be found that the introduction of CeO_2 can enhance the luminescence intensity of $MM'O_3$ and $MM'O_3$: Pr^{3+}.

Keywords Photoluminescence enhancement · Rare earth titanates · Cerium dioxide

Introduction

The investigation of luminescent properties of the rare earth elements hosted in several crystalline matrices such as metal oxides, oxysalts, metal–organic compounds and variety of semiconductor materials is strongly motivated because of their applications in optoelectronics devices and flat panel displays [1–2]. Among the development of semiconductor ceramics, materials with active optical properties such as photoluminescence (PL), electroluminescence, cathodeluminescence, non-linear optical or electro-optical properties may lead to new optoelectronic devices with superior performance [3, 4]. During the past decades, the luminescence of several types of semiconductor compounds have been extensively studied in ceramic samples or single crystals doped with rare-earth ions such as Eu^{3+}, Nd^{3+}, Er^{3+}, due to their potential optoelectronic applications [5, 6]. Alkali-earth metal titanates belong to the important functional ceramics materials such as piezoelectricity, electrooptic devices, semiconductor etc [7–9]. Lately, the study has begun to pay more attention to the optical properties, especially photoluminescence properties for these compounds doped with some photoactive central species because these perovskite-structure materials are attractive as host matrices for photoactive rare earth ions doping which can be expected to have great applications in integrated light-emission devices, field emission displays (FEDs), and all-solid compact laser devices operating in the blue-green region and positive temperature coefficient (PTC) resistors [10–14]. For instance, Bryknar et al. reported the low temperature laser excited luminescence of Mn-doped $SrTiO_3$ single-crystal [15]. Leite et al. discussed the nature of visible photoluminescence at room temperature in amorphous calcium titanate in the light of the results of recent experimental and quantum mechanical theoretical studies [16]. Yamamotoa et al. studied the luminescence of rare-earth ions in $SrTiO_3$ or other perovskite-type oxides and their use as a probe of physical properties of a host crystal [17]. Longo et al. furtherly prepared amorphous $SrTiO_3$ thin films by chemical solution

B. Yan (✉) · X. Cai · X. Xiao
Department of Chemistry, Tongji University,
Shanghai 200092, People's Republic of China
e-mail: byan@tongji.edu.cn

deposition and revealed an intense single-emission band in the visible region from the corresponding photoluminescence spectrum [18]. Beside this, some work has tried to substitute different metal ions (A or B) in these ABO_3 type lattice structure by using the similarity of physical properties [19–21]. The main discussion on the nature of the photoluminescence for these titanates may be related to the disordered structure in their ABO_3 materials. It is worthy pointing out that the room temperature photoluminescence behavior of amorphous titanate-type compounds doped rare earth ions, i.e. Pr^{3+}, has not yet been extensively studied except for some fragmentary work although they have great potential applications in optical display and energy conversion [22–28]. On the other hand, Al^{3+} has been found to enhance the luminescence of Pr^{3+} in titanate phosphors [29–31].

Cerium is an important rare earth element, which has considerable applications in functional materials. Ce^{3+} belongs to the important active center for blue emission in rare earth silicate or aluminate phosphors, besides, it can also act an energy transfer medium in the green phosphors to sensitize the luminescence of Tb^{3+}. The luminescence of Ce^{4+} is relatively little to be studied except that Sr_2CeO_4 possesses one-dimensional chains of edge-sharing CeO_6 octahedron and displays a broad band with a peak position at 475 nm ascribed to change -transfer transition Ce^{4+}-O^{2-} [32–35]. As we know, Ce^{4+} exhibits the similar physical properties to Ti^{4+} (Zr^{4+}), which make it develop some applications in the fields of optics and catalysis, so it can be predicted that Ce^{4+} can also be replaced Ti^{4+} (Zr^{4+}) in their oxysalts systems to some extent. In this paper, a modified sol-gel synthesis technology was afforded to prepare nanocomposite phosphors: $MM'O_3/CeO_2$ and $MM'O_3/CeO_2$: Pr^{3+} (M=Ca, Sr; M′=Ti, Zr) (M=Ca, Sr; M′=Ti, Zr). Rare earth (Ce or Pr) coordination polymers and poly ethyl glycol (PEG) were introduced in the course of sol-gel (hydrolysis and polycondensation) process of as titanium and zirconium sources, resulting in multicomponent hybrid precursors. The room-temperature photoluminescence for these phosphors were discussed in detail.

Experimental section

Starting materials

Rare earth oxides (Pr_6O_{11}, CeO_2) have the purity of over 99.99%. Tetra-n-butyl titanate and zirconium acetonate with purity higher than 98.0% were used as the source of titanate and zirconate; Alkali earth carbonates ($CaCO_3$,$SrCO_3$) (purity≥99.0%) were used for the calcium and strontium components, other reagents are all analytically pure. Rare earth oxides and alkalicarbonates were dissolved with excess concentrated nitric acid to covert to their nitrates completely. Among it was worthy pointing out that aqueous solution of hydrogen peroxides (30% concentration) were used to behave as reducer to dissolve Pr_6O_{11}.

Synthesis of $MM'O_3/CeO_2$ (M=Ca, Sr; M′=Ti, Zr)

0.201 g $CaCO_3$ (0.296 $SrCO_3$) (2 mmol) was dissolved with excess concentrated nitric acid to convert into calcium (strontium) nitrates completely. An appropriate amount of ortho hydroxylbenzoic acid (HOHBA) was dissolved in a little of ethanol solution, whose *p*H value was adjusted to about 6.5, then $Ce(NO_3)_3$ (2*x* mmol, *x*=0.02, 0.05, 0.10, 0.20, 0.50) solution was added of which the molar ratio of HOHBA: Ce^{3+} was 3.2. Different amounts of aqueous solutions of calcium nitrate were added into the above mixed solutions, stirring by introducing PEG and tetra-n-butyl titanate (or zirconium acetonate) (2(1-*x*) mmol). After heating and stirring, light-yellow sol was obtained and dried in an oven to age as gel. The hybrid precursors were calcinated in a resistance stove for 5 hours at 800 °C, light yellow solid powders were achieved. The typical procedure for the synthesis is represented in the following:

$$\begin{aligned} MCO_3 + \text{excess}\,HNO_3 &\longrightarrow M(NO_3)_2 + xCe(NO_3)_3 + 3.2x\,HOHBA + 3.2x\,NH_3H_2O \\ &\longrightarrow M(NO_3)_2 + Ce(OHBA)_3]_n + 5.0\,PEG + (2-x)\,Ti(OC_4H_9)_4\,(Zr(ACAC)_4) \\ &\longrightarrow MM'O_3/CeO_2 + CO_2\uparrow + H_2O\uparrow + NH_3\uparrow + NO_2\uparrow \\ (M = Ca,\ Sr, M' &= Ti,\ Zr) \end{aligned}$$

Synthesis of $MM'O_3/CeO_2$: Pr^{3+} (M=Ca, Sr; M′=Ti, Zr)

0.201 g $CaCO_3$ (0.296 $SrCO_3$) (2 mmol) was dissolved with excess concentrated nitric acid to convert into calcium (strontium) nitrates completely. An appropriate amount of ortho hydroxylbenzoic acid (HOHBA) was dissolved in a little of ethanol solution, whose *p*H value was adjusted to about 6.5, then $Ce(NO_3)_3$ (2*x* mmol, *x*=0.02, 0.05, 0.10, 0.20, 0.50) and $Pr(NO_3)_3$ (0.01 mmol) solution was added of which the molar ratio of HOHBA: (Ce^{3+}+Pr^{3+}) was 3.2. Different amounts of aqueous solutions of calcium nitrate were added into the above mixed solutions, stirring by

introducing PEG and tetra-n-butyl titanate (or zirconium acetonate) (2(1-x) mmol). After heating and stirring, light-yellow sol was obtained and dried in an oven to age as gel. The hybrid precursors were calcinated in a resistance stove for 5 hours at 800 °C, light yellow solid powders were achieved. The hybrid precursors were calcinated in a resistance stove for 5 hours at 800 °C, light yellow solid powders were achieved. The typical reaction scheme for the synthesis is represented in the following:

$$
\begin{aligned}
&MCO_3 + \text{excess}\, HNO_3 \\
&\longrightarrow M(NO_3)_2 + xCe(NO_3)_3 + 0.5\%\ Pr\,(NO_3) + 3.2x\,HOHBA + 3.2xNH_3H_2O \\
&\longrightarrow M(NO_3)_2 + Ce(OHBA)_3]_n + 0.5\%\,Pr(OHBA_3)_n\,5.0\,PEG + (2-x)\,Ti(OC_4H_9)_4\,\left(Zr(ACAC)_4\right) \\
&\longrightarrow MM'O_3/CeO_2 : 5\%\ Pr^{3+} + CO_2\uparrow + H_2O\uparrow + NH_3\uparrow + NO_2\uparrow \\
&(M = Ca,\ Sr, M' = Ti,\ Zr)
\end{aligned}
$$

Physical measurements

The particle size and microstructure were characterized by means of X-ray diffraction (XRD, Bruke, D8-Advance, 40 kV and 20 mA, CuKα) and scanning electronic microscopy (SEM, Philips XL-30). Excitation and emission spectra at room temperature were determined with a Perkin–Elmer LS-55 model fluorophotometer (excitation slit width=10 nm, emission width=2.5 nm).

Results and discussion

Figure 1 shows the selective XRD patterns for composite titanate phosphors: (A) $CaTiO_3/CeO_2$; (B) $CaTiO_3/CeO_2$: Pr^{3+}; (C) $SrTiO_3/CeO_2$ and (D) $SrTiO_3/CeO_2$: Pr^{3+}. Both of XRD patterns indicate that the resultant product of calcium titanate phosphors (A) and (B) are indexed to crystallize in the orthorhombic system with space group Pnma under high thermolysis temperature, in agreement with JCPDS (35–0734). While both $SrTiO_3/CeO_2$ (C) and $SrTiO_3/CeO_2$: Pr^{3+} (D) present the XRD pattern of indexing to crystallize in the cubic system with space group I4/mcm for strontium titanates under high thermolysis temperature of 800 °C, in agreement with JCPDS (35–0734), Both calcium and strotium titanates possess the single phase with certain structure. Besides, some doping rare earth ions can not affect the perovskite crystal structure of titanates. The diffraction peak appears broadening and the average crystallite size was estimated from the full width at half maximum of the diffraction peak by the Scherrer equation [29, 30]. From the estimated data, the particle sizes of these phosphors are found in the range of 29 nm. Figure 2 shows the XRD patterns for selected composite phosphors: (A) $CaZrO_3/CeO_2$; (B) $CaZrO_3/CeO_2$: Pr^{3+}; (C) $SrZrO_3/CeO_2$ and (D) $SrZrO_3/CeO_2$: Pr^{3+}. Both of XRD patterns indicate that the resultant product of calcium titanate phosphors (A) and (B) are indexed to crystallize in the cubic system in agreement with JCPDS (75–0358). While both $SrZrO_3/CeO_2$ (C) and $SrZrO_3/CeO_2$: Pr^{3+} (D) present the XRD pattern of indexing to crystallize in the orthorhombic cubic system for strontium titanates under high thermolysis temperature of 800 °C, in agreement with JCPDS (10 – 0268), both calcium and strotium titanates possess the single phase with certain structure. Besides, some doping rare earth ions can not affect the perovskite crystal structure of titanates. The diffraction peaks appear broadening and the average crystallite size was estimated from the full width at half maximum of the diffraction peak by the Scherrer equation [29, 30]. From the estimated data, the particle sizes of these phosphors are found in the range of 43 nm.

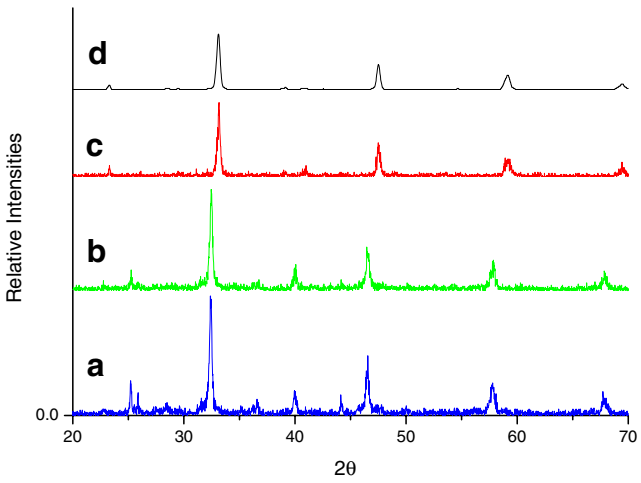

Fig. 1 XRD patterns for rare earth titanate phosphors: (*A*) $CaTiO_3/CeO_2$; (*B*) $CaTiO_3/CeO_2$: Pr^{3+}; (*C*) $SrTiO_3/CeO_2$ and (*D*) $SrTiO_3/CeO_2$: Pr^{3+}

Figure 3 shows the excitation spectra of $CaTiO_3/CeO_2$ and $SrTiO_3/CeO_2$ phosphors, respectively. Both series of these phosphors show apparent excitation in the narrow wavelength ultraviolet spectral bands (200~350 nm), especially a strong excitation peak with a maximum excitation peak around

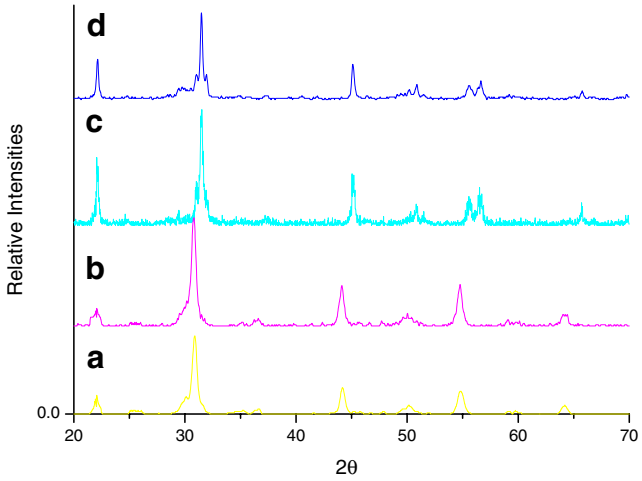

Fig. 2 XRD patterns for rare earth zirconate phosphors: (*A*) $CaZrO_3/CeO_2$; (*B*) $CaZrO_3/CeO_2$: Pr^{3+}; (*C*) $SrZrO_3/CeO_2$ and (*D*) $SrZrO_3/CeO_2$: Pr^{3+}

243 nm, which can be ascribed as the host absorption band. For Fig. 4 (A), under the excitation of 243 nm, $CaTiO_3/CeO_2$ exhibits a broad emission band (over 150 nm range) at 400 nm, corresponding to the host emission. The different composite content of CeO_2 can have some influences on the luminescent intensities of phosphors. At the range of 0.05–0.50 ratio of CeO_2, the luminescent intensities depend on the ratio of CeO_2 and $CaTiO_3/CeO_2$ phosphors show the strongest intensity at the ratio of CeO_2: $CaTiO_3$ of 0.05. We have not obtained if there exist some orderliness and relationship between the ratio of CeO_2 and the luminescent intensities. The deep research is underway. For Fig. 4 (B), $SrTiO_3/CeO_2$ exhibits a strong broad emission bands at 380 nm, which is attributed to the host emission. Similarly, the composition content of $CaTiO_3$ can modify the luminescent intensities of $SrTiO_3/CeO_2$ phosphors except that the content of $CaTiO_3$ for

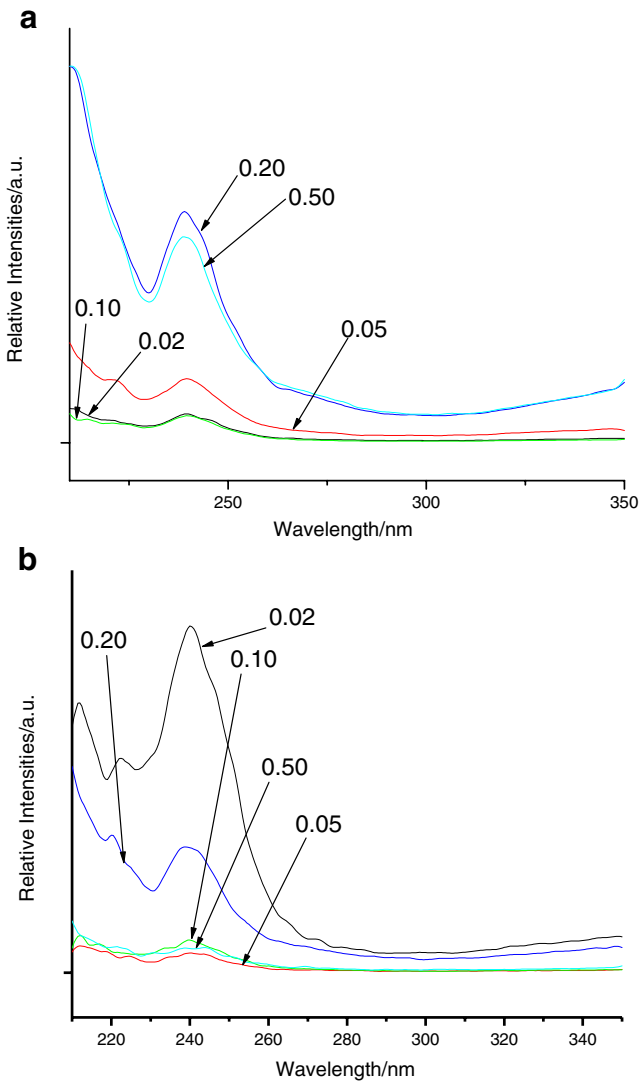

Fig. 3 Excitation spectra of $CaTiO_3/CeO_2$ (**a**) and $SrTiO_3/CeO_2$ (**b**) composites

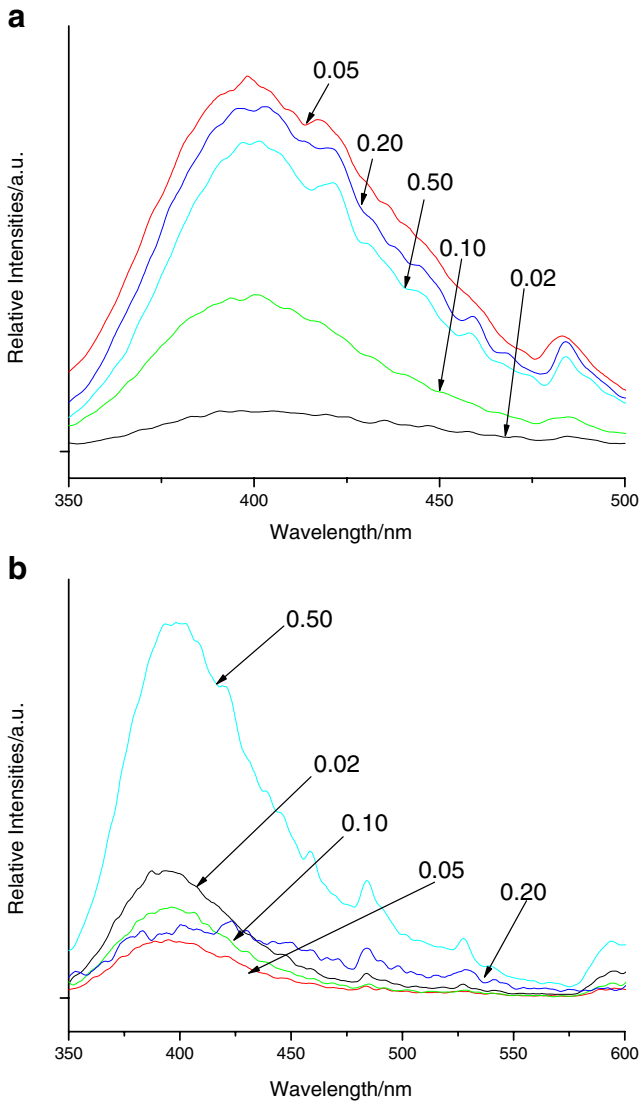

Fig. 4 Emission spectra of $CaTiO_3/CeO_2$ (**a**) and $SrTiO_3/CeO_2$ (**b**) composites

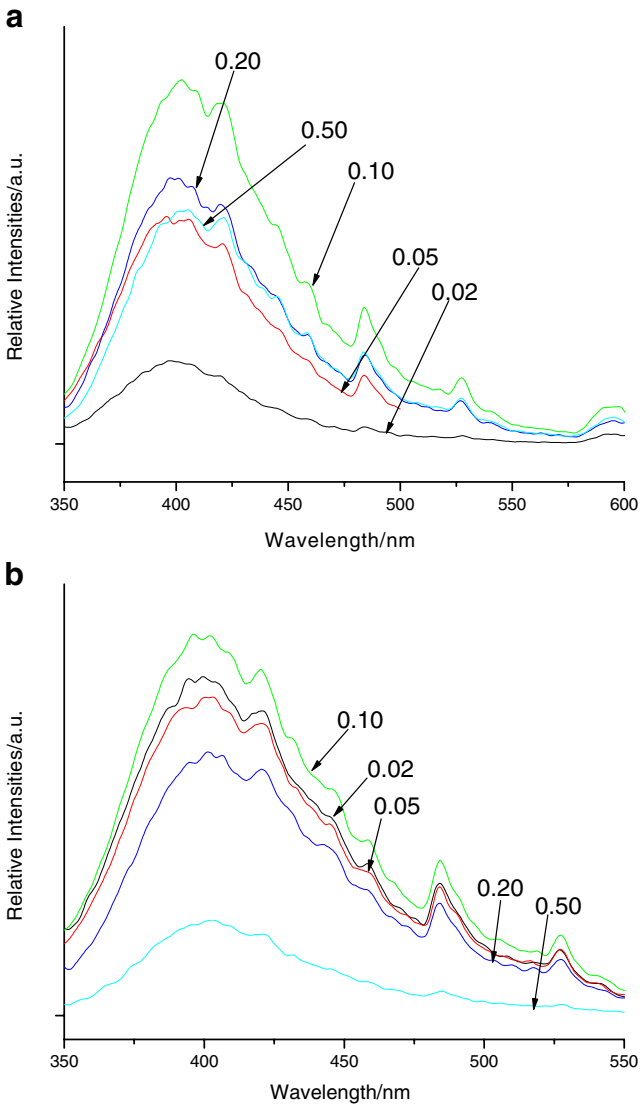

Fig. 5 Emission spectra of $CaZrO_3/CeO_2$ (**a**) and $SrZrO_3/CeO_2$ (**b**) composites

the strongest emission of $SrTiO_3/CeO_2$ is different (x=0.20). Both $SrTiO_3/CeO_2$ and $SrTiO_3/CeO_2$ phosphors indicate that $CaTiO_3$ can enhance the luminescence of titanate host and the enhancement effect of luminescence is related to the content of $CaTiO_3$ The same tetravalent Ti^{4+} and Ce^{4+} can not arise the electronic balance. Besides, CeO_2 can produce the effective absorption in the ultraviolet region and strong violet emission at around 380 to 400 nm, which is similar to the absorption and emission of host titanate framework (TiO_3^{2-}). Subsequently, the introduction of CeO_2 can improve the luminescence of calcium and strontium titanates. Certainly, it also can be predicted that only CeO_2 is situated at the certain content, the microstructure and coordination environment are suitable for the luminescence of $SrTiO_3/CeO_2$. Furthermore, this phenomenon is also related to the balance ion of Ca^{2+} and Sr^{2+} for the different radius to give rise to different local lattice surrounding. Figure 5 wears the excitation spectra of $CaZrO_3/CeO_2$ (A) and $SrZrO_3/CeO_2$ (B) phosphors. Both $CaZrO_3/CeO_2$ and $SrZrO_3/CeO_2$ exhibit the similar strong broad absorption band at around 400 nm, corresponding to the host emission. The different composition of CeO_2 can influence the luminescent intensities of zirconate phosphors. The content of CeO_2 for the highest emission of $CaZrO_3/CeO_2$ and $SrZrO_3/CeO_2$ are 0.10 and 0.20, respectively. CeO_2 can produce the effective absorption in the ultraviolet region and strong violet emission at around 400 nm, which is similar to the absorption and emission of host zirconate framework. Subsequently, the introduction of Ce^{4+} can improve the luminescence of calcium and strontium zirconate.

Figure 6 presents the emission spectra for $CaTiO_3/CeO_2$ and $CaZrO_3/CeO_2$ doping 0.5 mol % Pr^{3+} with different host composition ratio of CeO_2. Both series of these phosphors show no apparent excitation in the narrow

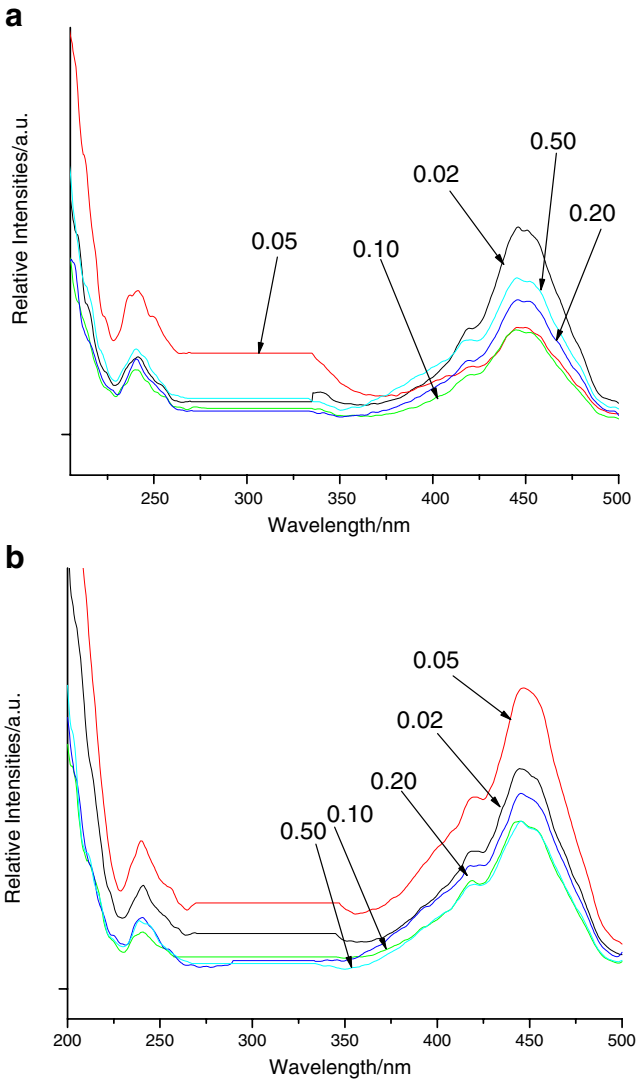

Fig. 6 Excitation spectra of $CaTiO_3/CeO_2$: Pr^{3+} (**a**) and $CaZrO_3/CeO_2$: Pr^{3+} (**b**) composites

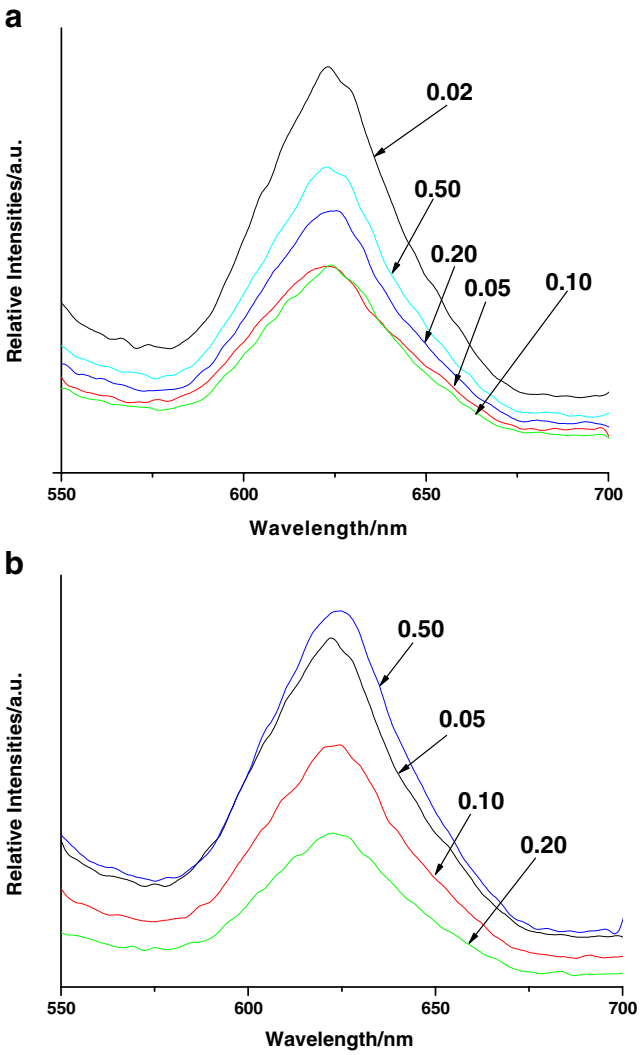

Fig. 7 Emission spectra of $CaTiO_3/CeO_2$: Pr^{3+} (**a**) and $SrTiO_3/CeO_2$: Pr^{3+} (**b**) composites

wavelength ultraviolet spectral bands (200~350 nm), while they exhibit distinct excitation bands in the long wavelength ultraviolet-visible region (350~500 nm), especially a strong excitation peak in blue-purple visible region with a maximum excitation peak around 449 nm for $CaTiO_3/CeO_2$: Pr^{3+} and $CaZrO_3/CeO_2$: Pr^{3+}. These wide excitation spectral bands are ascribed to the f → f transition absorption. The fact of strong excitation bands in visible region has a special significance as regards the expectation to realize the conversation of visible light. Under the excitation of 449 nm for $CaTiO_3/CeO_2$: Pr^{3+} (Fig. 7 (A)), the corresponding emission spectra for the series of phosphors show a strong broad emission band (about 50 nm range) in the range of 580~630 nm with a maximum peak at 620 nm for the $CaTiO_3/CeO_2$: Pr^{3+} phosphors. These emission bands originate from the characteristic $^1D_2 \rightarrow {}^3H_4$ transition of Pr^{3+}. Under the excitation of 449 nm for $SrTiO_3/CeO_2$: Pr^{3+} (Fig. 7 (B)), the corresponding emission spectra for the series of phosphors show a similar feature, presenting a strong broad emission band (about 50 nm range) in the range of 580~630 nm with a maximum peak at 619 nm for the $SrTiO_3/CeO_2$: Pr^{3+} phosphors. These emission bands originate from the characteristic $^1D_2 \rightarrow {}^3H_4$ transition of Pr^{3+}. The luminescence of Pr^{3+} has only a single series of spectra, which was ascribed to the praseodymium ions at the alkaline-earth site by comparison of ionic sizes [13]. The characteristic luminescence of these phosphors is determined by the electronic structure of the doped Pr^{3+}, while the width and the relative intensity of the spectra frequently depend on the crystal symmetry of the host matrix [13]. It is worthy pointing out that these phosphors present excitations in the blue-purple light range and emission in red light range, which can achieve light conversion in visible religion.

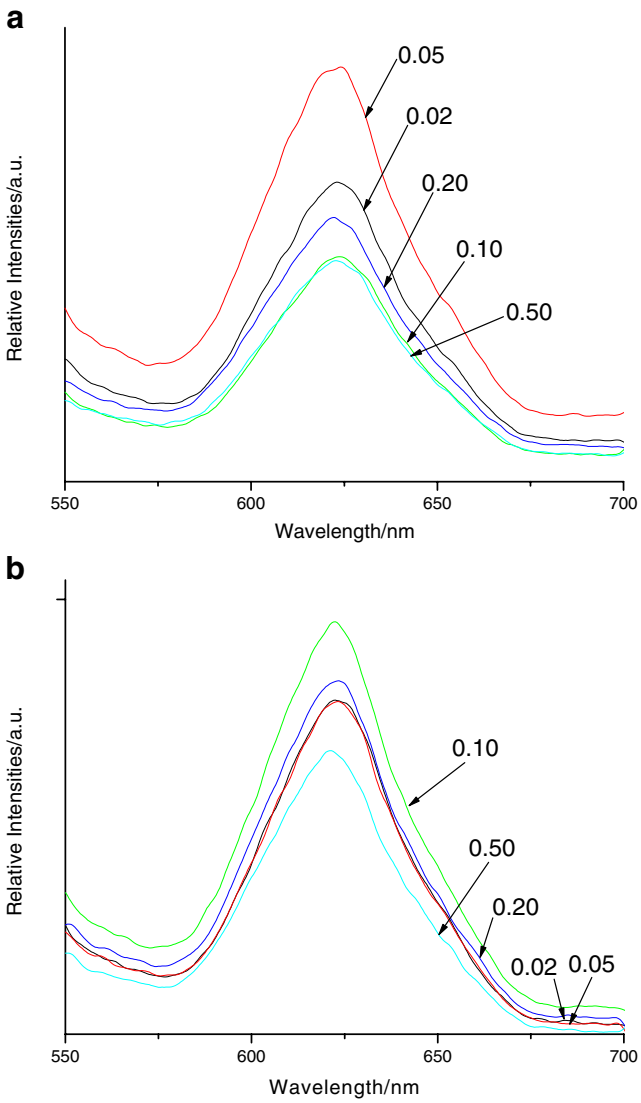

Fig. 8 Emission spectra of $CaZrO_3/CeO_2$: Pr^{3+} (**a**) and $SrZrO_3/CeO_2$: Pr^{3+} (**b**) composites

Compared the emission intensities for different composition ratio of CeO_2, it can be observed that different host composition has no great influence on the luminescent bands except for little distinction of luminescent intensities. Both of which wear the similar characteristics: the broad excitation band (400~550 nm) with maximum excitation peak of around 450 nm and the red emission band with maximum wavelength of about 620 nm. The luminescent intensities do not show evident difference and $SrTiO_3$/CeO_2: 3 mol % Pr^{3+} reaches the strongest. Both Ti and Zr form the BO_3 octahedron framework with oxygen atoms and both of them have the similar radius for the fact of Lanthanide Contraction, so different ratio of Ti and Zr has only little influence on the absorption of BO_3^{2-} and these phosphors with different composition of Zr/Ti ratio exhibit the luminescence of the same order. Under the excitation of 449 nm for $CaZrO_3/CeO_2$: Pr^{3+} (Fig. 8 (A)), the corresponding emission spectra for the series of phosphors show a strong broad emission band (about 50 nm range) in the range of 580~630 nm with a maximum peak at 620 nm for the $CaZrO_3/CeO_2$: Pr^{3+} phosphors. These emission bands originate from the characteristic $^1D_2 \rightarrow {}^3H_4$ transition of Pr^{3+}. Under the excitation of 449 nm for $SrZrO_3/CeO_2$: Pr^{3+} (Fig. 8 (B)), the corresponding emission spectra for the series of phosphors show a similar feature, presenting a strong broad emission band (about 50 nm range) in the range of 580~630 nm with a maximum peak at 619 nm for the $SrZrO_3/CeO_2$: Pr^{3+} phosphors. These emission bands originate from the characteristic $^1D_2 \rightarrow {}^3H_4$ transition of Pr^{3+}. The luminescence of Pr^{3+} has only a single series of spectra, which was ascribed to the praseodymium ions at the alkaline-earth site by comparison of ionic sizes [13]. The characteristic luminescence of these phosphors is determined by the electronic structure of the doped Pr^{3+}, while the width and the relative intensity of the spectra frequently depend on the crystal symmetry of the host matrix [13]. It is worthy pointing out that these phosphors present excitations in the blue-purple light range and emission in red light range, which can achieve light conversion in visible religion. Compared the emission intensities for different composite ratio of $SrTiO_3/CeO_2$ matrix, it can be observed that different host composition has no great influence on the luminescent bands except for little distinction of luminescent intensities. Both of which wear the similar characteristics: the broad excitation band (400~550 nm) with maximum excitation peak of around 450 nm and the red emission band with maximum wavelength of about 620 nm. The luminescent intensities do not show evident difference and $SrZrO_3/CeO_2$: 3 mol % Pr^{3+} reaches the strongest. Both Ti and Zr form the BO_3 octahedron framework with oxygen atoms and both of them have the similar radius for the fact of Lanthanide Contraction, so different ratio of Ti and Zr has only little influence on the absorption of BO_3^{2-} and these phosphors with different composition of Zr/Ti ratio exhibit the luminescence of the same order.

Conclusions

In summary, rare earth ceramic composite phosphors MM′O_3/CeO_2 and MM′O_3/CeO_2: Pr^{3+} (M=Ca, Sr; M′=Ti, Zr) are synthesized by a modified sol-gel process with multicomponent hybrid precursors, whose particle sizes are in the submicrometer range of 100~300 nm and the photoluminescence for these ceramic phosphors are studied in details with the different component of host (molecular ratio of Sr, Ca and Ti, Zr). The excitation spectra presented a broad spectral band in the visible blue-violet region with the maximum excitation peak at 449 nm, while no apparent absorption appeared in ultraviolet region. The corresponding emission spectra showed a wide emission range with a maximum peak at 619 nm. Which was ascribed to be the characteristic transition of Pr^{3+} ($^1D_2 \rightarrow {}^3H_4$), which can be expected for visible light conversion (blue → red) materials. Especially Ce^{4+} was introduced to replace Ti^{4+} or Zr^{4+} and the influence of CeO_2 on the photoluminescence of these phosphors were discussed. It can be found that CeO_2 can enhance the luminescence intensity of MM′O_3 and MM′O_3: Pr^{3+}.

Acknowledgements This work was supported by the Science Fund of Shanghai Universities for Excellent Youth Scientists and the National Natural Science Foundation of China (20671072).

References

1. Toyoda M, Hamaji Y, Tomoro K, Payne DA (1993) Ferroelectric properties and fatigue characteristics of Bi4Ti3O12 thin films by sol-gel processing. Jpn J Appl Phys 33:5543 doi:10.1143/JJAP.33.5543
2. Craciun V, Singh RK (2000) Characteristics of the surface layer of barium strontium titanate thin films deposited by laser ablation. Appl Phys Lett 76:1932 doi:10.1063/1.126216
3. Schwartz RN, Wechsler BA, West L (1995) Spectroscopic and photorefractive properties of molybdenum-doped barium-titanate. Appl Phys Lett 67:1352 doi:10.1063/1.115548
4. Rouma B, Blasse G (1995) Dependence of luminescence of titanates on their crystal structure. J Phys Chem Solids 56:261 doi:10.1016/0022-3697(94)00174-X
5. Ballato J, Esmacher R, Schwartz R, Dejneka M (2000) Phonon sideband spectroscopy and 1550 nm luminescence from Eu^{3+} and Er^{3+}-doped ferroelectric PLZT for active electro-optic applications. J Lumin 86:101 doi:10.1016/S0022-2313(99)00600-6
6. Liu H, Li ST, Liu GK, Jia W, Fernández FE (1999) Optical properties of undoped and Eu^{3+}-doped SBN thin film grown by pulsed laser deposition. J Lumin 83–84:367 doi:10.1016/S0022-2313(99)00127-1
7. Chen M, Liu ZL, Wang CC, Wang Y, Yang XS, Yao KL (2004) Temperature characteristics of electrical behavior of W-Bi-Ti-O

ceramics at low field. Chin Sci Bull 49:313 doi:10.1360/03WW0061
8. Bao DH, Wu XQ, Zhang LY, Yao X (1999) Preparation, electrical and optical properties of (Pb,Ca)TiO_3 thin films using a modified sol-gel technique. Thin Solid Films 350:30 doi:10.1016/S0040-6090(99)00273-4
9. Chopra S, Tripathi AK, Goel TC, Mendiratta RG (2003) Characterization of sol-gel synthesized lead calcium titanate (PCT) thin films for pyro-sensors. Mater Sci Eng B 100:180 doi:10.1016/S0921-5107(03)00095-3
10. Itoh S, Toki H, Tamura K, Kataoka F (1999) A new red-emitting phosphor, $SrTiO_3$: Pr^{3+}, for low-voltage electron excitation. Jpn J Appl Phys 36:6387 doi:10.1143/JJAP.38.6387
11. Pizani PS, Leite ER, Pontes FM, Paris EC, Rangel JH, Lee JH et al (2000) Photoluminescence of disordered ABO(3) perovskites. Appl Phys Lett 77:824 doi:10.1063/1.1306663
12. Okamoto S, Yamamoto H (2001) Characteristic enhancement of emission from $SrTiO_3$: Pr^{3+} by addition of group-IIIb ions. Appl Phys Lett 78:655 doi:10.1063/1.1343491
13. Zhang HX, Kam CH, Zhou Y, Han XQ, Buddhudu S, Xiang Q et al (2000) Green upconversion luminescence in Er^{3+}: $BaTiO_3$ films. Appl Phys Lett 77:609 doi:10.1063/1.127060
14. Gedanken A, Reisfeld R, Sominski L, Zhong Z, Koltypin Y, Panczer G et al (2000) Time-dependence of luminescence of nanoparticles of Eu2O3 and Tb2O3 deposited on and doped in alumina. Appl Phys Lett 77:945 doi:10.1063/1.1289068
15. Bryknar Z, Trepakov V, Potucek Z, Jastrabik L (2000) Luminescence spectra of $SrTiO_3$: Mn^{4+}. J Lumin 87–89:605 doi:10.1016/S0022-2313(99)00325-7
16. Pontes FM, Pinheiro CD, Longo E, Leite ER, de Lazaro SR, Varela JA et al (2002) The role of network modifiers in the creation of photoluminescence in $CaTiO_3$. Mater Chem Phys 78:227 doi:10.1016/S0254-0584(02)00230-4
17. Yamamoto H, Okamoto S, Kobayashi H (2002) Luminescence of rare-earth ions in perovskite-type oxides: from basic research to applications. J Lumin 100:325 doi:10.1016/S0022-2313(02)00432-5
18. Pontes FM, Longo E, Leite ER, Lee EJH, Varela JA, Pizani PS et al (2002) Photoluminescence at room temperature in amorphous SrTiO3 thin films obtained by chemical solution deposition. Mater Chem Phys 77:598 doi:10.1016/S0254-0584(02)00112-8
19. Soe KKK, Maeda M, Suzuki I (1996) Sol-gel processing of $Pb_{1-x}Ca_xTiO_3$ thin films. Mater Lett 27:373 doi:10.1016/0167-577X(96)00021-3
20. Samantaray CB, Goswami MLN, Bhattacharya D, Ray SK, Acharya HN (2004) Photoluminescence properties of Eu^{3+}-doped barium strontium titanate (Ba, Sr)TiO_3 ceramics. Mater Lett 58:2299 doi:10.1016/S0167-577X(04)00124-7
21. Vashook V, Vasylechko L, Knapp M, Ullmann H, Guth U (2003) Lanthanum doped calcium titanates: synthesis, crystal structure, thermal expansion and transport properties. J Alloy Comp 354:13 doi:10.1016/S0925-8388(02)01345-2
22. Park JK, Ryu H, Park HD, Choi SY (2001) Synthesis of $SrTiO_3$: Al, Pr phosphors from a complex precursor polymer and their luminescent properties. J Eur Ceram Soc 21:535 doi:10.1016/S0955-2219(00)00238-7
23. Okamoto S, Kobayashi H, Yamamoto H (1999) Enhancement of characteristic red emission from $SrTiO_3$: Pr^{3+} by Al addition. J Appl Phys 86:5594 doi:10.1063/1.371565
24. Diallo PT, Boutinaud P, Mahiou R, Cousseins JC (1997) Red luminescence in Pr^{3+}-doped calcium titanates. Phys Status Solidi 160:255 doi:10.1002/1521-396X(199703)160:1<255::AID-PSSA255>3.0.CO;2-Y
25. Boutinaud P, Pinel E, Dubois M, Vink AP, Mahiou R (2005) UV-to-red relaxation pathways in $CaTiO_3$: Pr^{3+}. J Lumin 111:69 doi:10.1016/j.jlumin.2004.06.006
26. Kim JS, Choi JH, Cheon CI, Byun JD (2004) Luminescence characteristics of $SrTiO_3$: Pr, Ga phosphor synthesized by sol-gel process. Ceram Int 30:2029 doi:10.1016/j.ceramint.2003.12.200
27. Yan B, Zhou K (2005) In-situ sol-gel composition of inorganic/organic polymeric hybrid precursors to synthesize red-luminescent $CaTiO_3$: Pr^{3+} and $CaTi_{0.5}Zr_{0.5}O_3$: Pr^{3+} phosphors. J Alloy Comp 398:165 doi:10.1016/j.jallcom.2004.08.109
28. Yan B, Zhou K (2004) In-situ sol-gel composition of hybrid precursors to synthesize $SrTiO_3$: Pr^{3+} red ceramic phosphors. J Rare Earths 22:272
29. Matsushita N, Tsuchiya N, Nakatsuka K, Yanagitani T (1999) Precipitation and calcination processes for yttrium aluminum garnet precursors synthesized by the urea method. J Am Ceram Soc 82:1977
30. Zhang JJ, Ning JW, Liu XJ, Pan YB, Huang LP (2003) A novel synthesis of phase-pure ultrafine YAG: Tb phosphor with different Tb concentration. Mater Lett 57:3077 doi:10.1016/S0167-577X(02)01439-8
31. Orhan E, Pontes FM, Pinheiro CD, Boschi TM, Leite ER, Pizani PS et al (2004) Origin of photo luminescence in SrTiO3: a combined experimental and theoretical study. J Solid State Chem 177:3879 doi:10.1016/j.jssc.2004.07.043
32. Danielson E, Devenney M, Giaquinta DM, Haushalter RC, McFarland EW, Poojary DM et al (1998) A rare earth phosphor containing one-dimensional chains identified through combinatorial methods. Science 279:837 doi:10.1126/science.279.5352.837
33. Danielson E, Devenney M, Giaquinta DM, Haushalter RC, McFarland EW, Poojary DM et al (1998) X-ray powder structure of Sr_2CeO_4: a new luminescent material discovered by combinatorial chemistry. J Mol Struct 470:229 doi:10.1016/S0022-2860(98)00485-2
34. Jiang YD, Zhang FL, Summers CD, Wang ZL (1999) Synthesis and properties of Sr_2CeO_4 blue emission powder phosphor for field emission displays. Appl Phys Lett 72:1677 doi:10.1063/1.123652
35. Lee YE, Nortor DP, Budai JD, Rack PD, Potter MD (2000) Photo and cathodeluminescence characteristics of blue light emitting epitaxial Sr_2CeO_4 thin film phosphors. Appl Phys Lett 77:678 doi:10.1063/1.127083